

Dosimetric Properties of Ce-doped 25Li₂O–10MgO–65SiO₂ Glasses

Kensei Ichiba,* Yuma Takebuchi, Hiromi Kimura, Daiki Shiratori,
Takumi Kato, Daisuke Nakauchi, Noriaki Kawaguchi, and Takayuki Yanagida

Nara Institute of Science and Technology, 8916-5 Talayama-cho, Ikoma, Nara 630-0192, Japan

(Received October 6, 2021; accepted October 28, 2021)

Keywords: dosimeter, TSL, glass, storage phosphor

We prepared 25Li₂O–10MgO–65SiO₂ glasses doped with various concentrations of Ce by the melt-quenching method and systematically evaluated their photoluminescence (PL) and dosimetric properties. X-ray diffraction patterns showed that the prepared samples were in an amorphous state. The PL spectra and decay curves of the Ce-doped glasses confirmed the PL emission peak due to the 5d–4f transitions of Ce³⁺ ions. The PL quantum yields of the 0.3, 1, 3, 5, and 10% Ce-doped glasses were 17.5, 31.0, 36.6, 27.2, and 26.3%, respectively. Regarding dosimetric properties, the Ce-doped glasses showed thermally stimulated luminescence (TSL) at 100, 300, and 400 °C. Moreover, the 1, 3, 5, and 10% Ce-doped glasses showed the TSL dose response from 10 mGy to 10 Gy with a proportional relationship.

1. Introduction

Dosimeters using storage phosphors can retain the information of radiation dose and have been used in various fields such as personal dosimetry^(1,2) and medical imaging.^(3,4) The luminescence mechanism of storage phosphors is that, first, many carriers generated by radiation are captured at localized trapping centers. Then, these trapped carriers are released following an external stimulation, and finally, photons are emitted by the recombination of carriers at luminescence centers. The types of luminescence caused by light and heat stimulations are called optically stimulated luminescence (OSL) and thermally stimulated luminescence (TSL), respectively.^(5,6) Furthermore, there is another type of luminescence called radiophotoluminescence (RPL).^(7,8) In this case, localized trapping centers generated by radiation act as luminescence centers, unlike OSL and TSL. The storage phosphors for personal dosimetry require a high luminescence intensity, dose linearity, and effective atomic number (Z_{eff}) close to that of human soft tissue ($Z_{eff} = 7.29$).

To date, there have been many reports on the dosimetric properties of various material forms such as ceramics, single crystals, and glasses.^(9–19) Among these material forms, glasses have attracted considerable attention because of their low cost, large productivities, easy handling, and multiple chemical compositions. However, reports on the dosimetric properties of glass

*Corresponding author: e-mail: ichiba.kensei.if7@ms.naist.jp
<https://doi.org/10.18494/SAM3680>

materials are few, and only Ag-doped phosphate glass has been commercially available as an RPL dosimeter;⁽²⁰⁾ therefore, there still remains room for research on glass dosimeters.

In this study, we focused on SiO₂-based glasses in order to develop suitable materials for personal dosimetry. Thus far, SiO₂-based glasses have attracted much attention as phosphors because they have good thermal stability, chemical stability, and optical properties.⁽²¹⁾ In the radiation measurement fields, SiO₂-based glasses, including activator-doped SiO₂, Li₂O–MgO–Al₂O₃–SiO₂, SrO–Al₂O₃–SiO₂, and Li glasses (Saint-Gobain), have been reported.^(21–26) Among the SiO₂-based glasses, the 25Li₂O–10MgO–65SiO₂ glasses have been studied as the scintillator for neutron detectors;⁽²⁷⁾ however, no research on their dosimetric properties has been done, to the best of our knowledge. This glass composition is the suitable storage phosphor for personal dosimetry because the Z_{eff} of 25Li₂O–10MgO–65SiO₂ glasses ($Z_{\text{eff}} = 11.3$) is close to that of human soft tissue. For the above reasons, we synthesized 25Li₂O–10MgO–65SiO₂ with various concentrations of Ce by the melt-quenching method, and their photoluminescence (PL) and dosimetric properties were systematically surveyed.

2. Materials and Methods

Undoped and Ce-doped 25Li₂O–10MgO–65SiO₂ glasses were synthesized by the conventional melt-quenching method. Li₂CO₃ (99.99%, Rare Metallic), MgCO₃ (99.99%, High Purity Chemicals), and SiO₂ (99.99%, Rare Metallic) as starting materials were mixed at the molar ratio of 25:10:65. To study the dopant concentration dependence on PL and dosimetric properties, CeO₂ (99.99%, Furuuchi Chemical) was added. The nominal concentrations of CeO₂ were 0.3, 1, 3, 5, and 10% with respect to the host. These powders were weighed in a total amount of 10 g and mixed with agate mortar until homogeneous. The mixtures were transferred to alumina crucibles, then melted in an electric furnace at 1400 °C for 60 min in air ambient, and the melt was quenched on a stainless-steel plate preheated to 200 °C. After sufficient cooling, a polishing machine (Buehler, MetaServ 250) was used to mechanically polish the surface of the samples. To determine if the obtained samples were amorphous, X-ray diffraction (XRD) pattern measurements were conducted in the range of 3–60° with a diffractometer (Rigaku, MiniFlex600). The in-line transmittance spectra were evaluated using a spectrophotometer (JASCO, V670) in the spectral range from 200 to 700 nm at 1 nm steps.

The PL excitation and emission spectra and quantum yield (QY) were obtained using Quantaaurus-QY (Hamamatsu, C11347-01). To identify the origin of PL, the PL decay time constants were evaluated using Quantaaurus- τ (Hamamatsu, C11367).

To elucidate the properties of Ce-doped glasses as the TSL dosimeter, TSL glow curves were measured with a TSL reader (NanoGray Inc., TL-2000)⁽⁵⁾ within 30 s after X-ray irradiation using an X-ray generator (Spellman, XRB80N100/CB). The measurements were undertaken at a heating rate of 1 °C/s and a temperature range from 50 to 490 °C. Moreover, after X-ray irradiation of the samples at a dose of 10 Gy, TSL spectra were measured using a CCD-based spectrometer (Ocean Optics, QE Pro) while heating the samples using an electric heater (Sakaguchi, SCR-SHQ-A).^(28,29) To evaluate the TSL dose response functions, we measured the TSL glow curves with different X-ray irradiation doses of 1 mGy to 10 Gy at 10-fold increments.

Dose rates for 1–10 mGy, 100 mGy, and 1–10 Gy were 0.6, 6, and 60 Gy/h, respectively. The dose response was defined as the integrated TSL intensity for each irradiation dose, and the intensities of the glow curves were corrected using the weight of each glass.

3. Results and Discussion

Figure 1 shows the XRD patterns of the undoped and Ce-doped 25Li₂O–10MgO–65SiO₂ glasses. A typical halo peak was shown in all the samples at the range of 15–35°, and the measured XRD patterns showed no crystalline phases. Therefore, the synthesized samples in this study were amorphous.

Figure 2 shows the in-line transmittance spectra of the undoped and Ce-doped glasses. The inset shows photographs of the glass samples after polishing to approximately 1 mm thickness. The weights of the undoped, 0.3, 1, 3, 5, and 10% Ce-doped glasses were 208.1, 66.6, 164.7, 89.5, 237.2, and 111.2 mg, respectively. All the glasses showed high transparency over the 350–700 nm range, which was consistent with their appearance as shown in the inset of Fig. 2. The undoped glass had the absorption edge at around 250 nm, which shifted to a longer wavelength with increasing Ce concentration. This shift was probably caused by both the 4f–5d absorption of Ce³⁺ and the charge-transfer absorption of Ce⁴⁺ because the absorption bands are close.^(30–34)

Figure 3(a) shows the PL excitation and emission spectrum of the 3% Ce-doped glass as a representative. The 3% Ce-doped glass showed the emission band at around 360 nm under the excitation at 320 nm. All the other Ce-doped samples showed a similar spectral feature but with different intensities. In the undoped glass, the emission band was not confirmed within the present excitation range. The *QY* values of the 0.3, 1, 3, 5, and 10% Ce-doped glasses were 17.5, 31.0, 36.6, 27.2, and 26.3%, respectively. When we compared with other Ce-doped SiO₂-based glasses, the *QY* value of the 3% Ce-doped glass was higher than those of some glasses, although lower than that of the commercially available Ce-doped Li glass (GS20).^(24,25,35) In addition, the

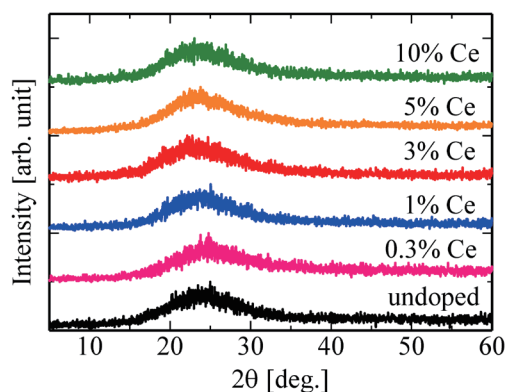


Fig. 1. (Color online) XRD patterns of undoped and Ce-doped samples.

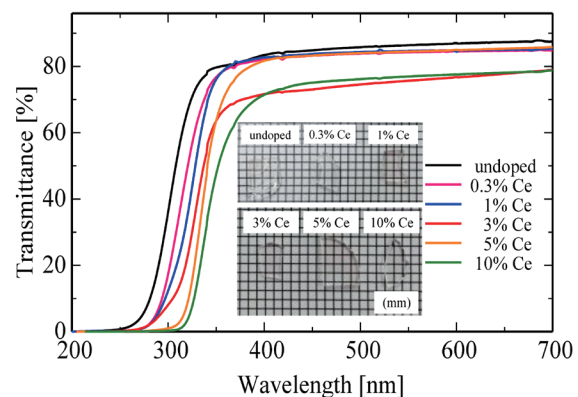


Fig. 2. (Color online) In-line transmittance spectra of undoped and Ce-doped glasses. The inset shows photographs of the glass samples.

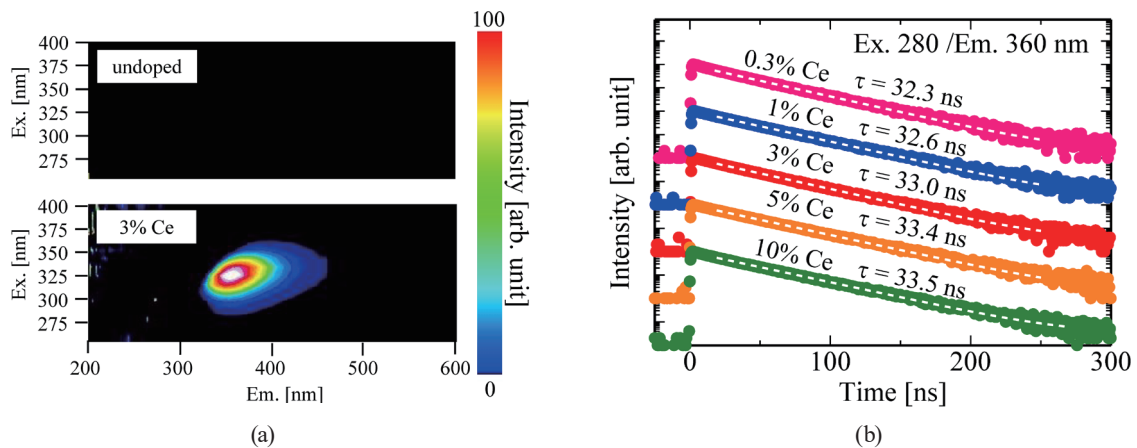


Fig. 3. (Color online) (a) PL excitation and emission spectra of undoped and 3% Ce-doped glasses. The horizontal and vertical axes show emission and excitation wavelengths, respectively. (b) PL decay curves of Ce-doped glasses. The excitation and monitoring wavelengths were 280 and 360 nm, respectively. Each of the dashed lines shows a fitting curve.

decrease in the QY value of the glasses doped with Ce higher than 3% would be caused by the concentration quenching.

Figure 3(b) shows the PL decay curves of the Ce-doped glasses monitored at 360 nm under the excitation of 280 nm. All the decay curves that excluded instrumental response functions were in agreement with a single exponential function. The decay time constants of the 0.3, 1, 3, 5, and 10% Ce-doped glasses were 32.3, 32.6, 33.0, 33.4, and 33.5 ns, respectively. All the decay time constants correspond to the typical value of the 5d–4f transitions of Ce^{3+} .^(36–39) Judging from both PL emission wavelength and decay time constants, the luminescence origin in the Ce-doped glasses is the 5d–4f transitions of Ce^{3+} .

Figure 4(a) shows the TSL glow curves of the undoped and Ce-doped glasses after X-ray irradiation of 1 Gy. Because the TSL intensity is proportional to the sample size, the TSL intensities in Fig. 4 were corrected using the weight of each glass. In the undoped glass, the TSL glow peak at around 100 °C was observed, although no emission bands were detected in PL. On the other hand, similar glow peaks were reported in previous studies of the other SiO_2 -based glasses.^(40–42) In the Ce-doped glasses, the glow peaks were confirmed at around 100, 300, and 400 °C. The trapping center of the glow peak at 100 °C in the Ce-doped glasses would be the same as that in the undoped glass. The two glow peaks at around 300 and 400 °C were detected in only the Ce-doped glasses, and the TSL intensities depended on the Ce concentration; thus, these glow peaks relate to trapping centers derived from Ce doping.

Figure 4(b) shows the TSL spectrum of the 10% Ce-doped glass as a representative of all the Ce-doped glasses. After X-ray irradiation of 10 Gy, the 10% Ce-doped glass was heated at 100 °C during the measurement. The TSL spectrum of the undoped glass was not observed because the TSL intensity was too low to measure with our instrument. The 10% Ce-doped glass showed the emission peak at 380 nm, which was also observed in the PL spectra. Therefore, Ce^{3+} ions act as the luminescence center in the TSL process.

Figure 5 shows the TSL dose response functions of the undoped and Ce-doped glasses. To assess the dose response functions, the TSL intensities of the glow curves were integrated into a

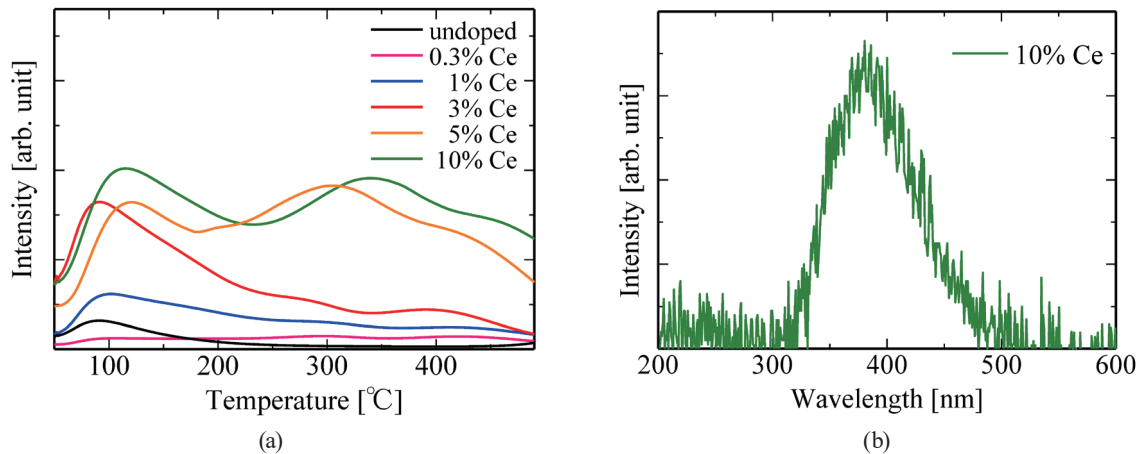


Fig. 4. (Color online) (a) TSL glow curves of undoped and Ce-doped glasses after X-ray irradiation of 1 Gy and (b) TSL spectrum of 10% Ce-doped glass heated at 100 °C after X-ray irradiation of 10 Gy. The intensities of the glow curves were corrected using the weight of each glass.

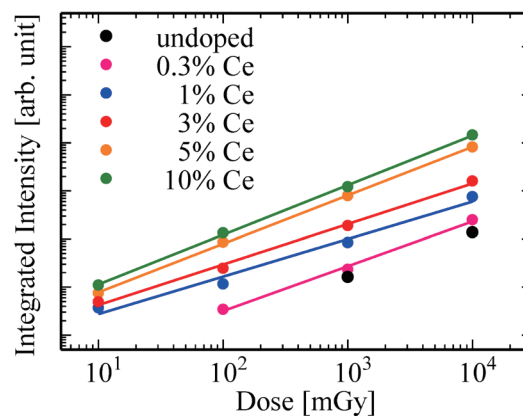


Fig. 5. (Color online) TSL dose response functions of undoped and Ce-doped glasses.

temperature range from 50 to 490 °C. As a result, the 1, 3, 5, and 10% Ce-doped glasses showed a proportional relationship from 10 mGy to 10 Gy. The coefficients of determination of the 0.3, 1, 3, 5, and 10% Ce-doped glasses were 0.996, 0.980, 0.996, 0.998, and 0.998, respectively. Therefore, the approximate functions were extremely accurate. In addition, the 10% Ce-doped glass showed the highest intensity among all the samples, which had no dependence on QY . The X-ray absorption efficiency of the glasses increased with increasing Ce concentration because of the increase in the Z_{eff} caused by Ce doping. Note that the Z_{eff} values of the undoped, 0.3, 1, 3, 5, and 10% Ce-doped samples are 11.3, 15.6, 20.4, 26.9, 30.6, and 36.1, respectively. The Z_{eff} values of the 0.3 and 1% Ce-doped glasses are closer to that of human soft tissue than those of some of the commercially available dosimetric materials.^(43,44) However, the lower detection limits were worse than those of commercially available dosimetric materials, which were 10–100 μGy . In future works, doping of different rare-earth ions or changing the glass composition is expected to improve the TSL intensity and sensitivity.

4. Conclusion

Undoped and Ce-doped 25Li₂O–10MgO–65SiO₂ glasses were synthesized by the melt-quenching method, and their PL and dosimetric properties were investigated. Regarding the PL properties, a broad emission peak due to the 5d–4f transitions of Ce³⁺ ions was observed in the Ce-doped glasses. The Ce-doped glasses also showed TSL, which was derived from the 5d–4f transitions of Ce³⁺. Moreover, the 1, 3, 5, and 10% Ce-doped glasses showed TSL with a linear response from 10 mGy to 10 Gy.

Acknowledgments

This work was supported by Grants-in-Aid for Scientific Research B (19H03533, 21H03733, and 21H03736) and Early-Career Scientists (20K15026 and 20K20104) from the Japan Society for the Promotion of Science. The Cooperative Research Project of the Research Center for Biomedical Engineering, Yashima Environment Technology Foundation, Okura Kazuchika Foundation, and Hitachi Metals-Materials Science Foundation are also acknowledged.

References

- 1 H. Nanto: *Sens. Mater.* **30** (2018) 327.
- 2 R. Oh, S. Yanagisawa, H. Tanaka, T. Takata, G. Wakabayashi, M. Tanaka, N. Sugioka, Y. Koba, and K. Shinsho: *Sens. Mater.* **33** (2021) 2129.
- 3 P. Leblans, D. Vandembroucke, and P. Willems: *Materials* **4** (2011) 1034.
- 4 C. M. Schaefer-Prokop and M. Prokop: *Eur. Radiol.* **7** (1997) S58.
- 5 T. Yanagida, Y. Fujimoto, N. Kawaguchi, and S. Yanagida: *J. Ceram. Soc. Jpn.* **121** (2013) 988.
- 6 T. Yanagida, G. Okada, and N. Kawaguchi: *J. Lumin.* **207** (2019) 14.
- 7 T. Yanagida: *Proc. Jpn Acad. Ser. B* **94** (2018) 75.
- 8 T. Kato, D. Shiratori, M. Iwao, H. Takase, D. Nakauchi, N. Kawaguchi, and T. Yanagida: *Sens. Mater.* **33** (2021) 2163.
- 9 H. Kimura, T. Kato, D. Nakauchi, N. Kawaguchi, and T. Yanagida: *Sens. Mater.* **33** (2021) 2187.
- 10 V. Altunal, V. Guckan, A. Ozdemir, and Z. Yegingil: *J. Alloys Compd.* **817** (2020) 152809.
- 11 H. Masai, H. Kimura, N. Kawaguchi, T. Yanagida, and N. Kitamura: *Radiat. Meas.* **135** (2020) 106344.
- 12 Y. Takebuchi, H. Fukushima, T. Kato, D. Nakauchi, N. Kawaguchi, and T. Yanagida: *Radiat. Phys. Chem.* **177** (2020) 109163.
- 13 H. Mizuno, T. Kanai, Y. Kusano, S. Ko, M. Ono, A. Fukumura, K. Abe, K. Nishizawa, M. Shimbo, S. Sakata, S. Ishikura, and H. Ikeda: *Radiother. Oncol.* **86** (2008) 258.
- 14 H. Kimura, T. Kato, D. Nakauchi, G. Okada, N. Kawaguchi, and T. Yanagida: *Nucl. Instrum. Methods Phys. Res., Sect. A* **954** (2020) 161226.
- 15 Y. Takebuchi, H. Fukushima, T. Kato, D. Nakauchi, N. Kawaguchi, and T. Yanagida: *Sens. Mater.* **32** (2020) 1405.
- 16 T. Kato, D. Nakauchi, N. Kawaguchi, and T. Yanagida: *Sens. Mater.* **32** (2020) 1411.
- 17 N. Kawaguchi, G. Okada, Y. Futami, D. Nakauchi, T. Kato, and T. Yanagida: *Sens. Mater.* **32** (2020) 1419.
- 18 N. Kawaguchi, H. Kimura, D. Nakauchi, T. Kato, and T. Yanagida: *J. Ceram. Soc. Jpn.* **129** (2021) 21005.
- 19 Y. Onoda, H. Kimura, T. Kato, K. Fukuda, N. Kawaguchi, and T. Yanagida: *Optik* **181** (2019) 50.
- 20 Y. Miyamoto, T. Yamamoto, K. Kinoshita, S. Koyama, Y. Takei, H. Nanto, Y. Shimotsuma, M. Sakakura, K. Miura, and K. Hirao: *Radiat. Meas.* **45** (2010) 546.
- 21 D. Shiratori, H. Kimura, D. Nakauchi, T. Kato, N. Kawaguchi, and T. Yanagida: *Radiat. Meas.* **134** (2020) 106297.
- 22 Y. Isokawa, H. Kimura, T. Kato, N. Kawaguchi, and T. Yanagida: *Opt. Mater.* **90** (2019) 187.
- 23 K. Hashimoto, D. Shiratori, T. Matsuo, T. Kato, D. Nakauchi, N. Kawaguchi, and T. Yanagida: *J. Mater. Sci. Mater. Electron.* **31** (2020) 17755.

- 24 T. Yanagida, J. Ueda, H. Masai, Y. Fujimoto, and S. Tanabe: *J. Non-Cryst. Solids* **431** (2016) 140.
- 25 H. Kimura, H. Masai, T. Kato, D. Nakauchi, N. Kawaguchi, and T. Yanagida: *J. Mater. Sci. Mater. Electron.* **31** (2020) 3017.
- 26 G. Okada, N. Kawaguchi, and T. Yanagida: *Opt. Mater.* **87** (2019) 84.
- 27 B. V. Shul'gin: *Phys. Solid State* **47** (2005) 1412.
- 28 G. Okada, T. Kato, D. Nakauchi, K. Fukuda, and T. Yanagida: *Sens. Mater.* **28** (2016) 897.
- 29 G. Okada, N. Kawaguchi, and T. Yanagida: *Opt. Mater.* **87** (2019) 84.
- 30 K. Ichiba, Y. Takebuchi, H. Kimura, T. Kato, D. Nakauchi, N. Kawaguchi, and T. Yanagida: *J. Mater. Sci.: Mater. Electron.* **32** (2021) 25065.
- 31 Y. Takebuchi, K. Watanabe, D. Nakauchi, H. Fukushima, T. Kato, N. Kawaguchi, and T. Yanagida: *J. Ceram. Soc. Jpn.* **129** (2021) 20233.
- 32 H. Kimura, K. Shinozaki, G. Okada, N. Kawaguchi, and T. Yanagida: *J. Non-Cryst. Solids* **508** (2019) 46.
- 33 M. Jia, J. Wen, W. Luo, Y. Dong, F. Pang, Z. Chen, G. Peng, and T. Wang: *J. Lumin.* **221** (2020) 117063.
- 34 T. Murata, M. Sato, H. Yoshida, and K. Morinaga: *J. Non-Cryst. Solids* **351** (2005) 312.
- 35 Y. Isokawa, D. Nakauchi, G. Okada, N. Kawaguchi, and T. Yanagida: *J. Alloys Compd.* **782** (2019) 859.
- 36 S. Matsumoto, A. Minamino, and A. Ito: *Sens. Mater.* **33** (2021) 2209.
- 37 T. Kato, G. Okada, N. Kawaguchi, and T. Yanagida: *J. Lumin.* **192** (2017) 316.
- 38 H. Feng, D. Ding, H. Li, S. Lu, S. Pan, X. Chen, and G. Ren: *J. Alloys Compd.* **489** (2010) 645.
- 39 D. Shiratori, D. Nakauchi, T. Kato, N. Kawaguchi, and T. Yanagida: *Sens. Mater.* **32** (2020) 1365.
- 40 G. Okada, S. Kasap, and T. Yanagida: *Opt. Mater.* **61** (2016) 15.
- 41 Y. Isokawa, D. Nakauchi, G. Okada, N. Kawaguchi, and T. Yanagida: *J. Alloys Compd.* **782** (2019) 859.
- 42 K. Hashimoto, D. Shiratori, D. Nakauchi, T. Kato, N. Kawaguchi, and T. Yanagida: *J. Ceram. Soc. Jpn* **128** (2020) 267.
- 43 V. E. Kafadar and K. F. Majeed: *Thermochim. Acta* **590** (2014) 266.
- 44 V. E. Kafadar, A. Necmeddin Yazici, and R. Güler Yildirim: *Nucl. Instrum. Methods Phys. Res., Sect. B* **267** (2009) 3337.